Precompound evaporation analyses of excitation functions for (α,xn) reactions

M. Blann and T. T. Komoto
University of California, Lawrence Livermore National Laboratory, Livermore, California 94550
(Received 20 June 1983)

Calculated (α,xn) excitation functions ($x=1$ to 4) for ^{233,234,235}U and ^{237}Np targets, for incident ^{4}He energies to 45 MeV, have been compared with experimental results. Calculations used experimental fission barriers with single particle ratios which were deduced by fitting experimentally deduced fission probabilities at excitations up to 12 MeV. Standard precompound parameters used for fitting spectra of nucleon-induced reactions were used, changing only the initial exciton number to four, appropriate for α-induced reactions. Agreement with experimental results was good to excellent, without the need of multiple precompound decay, nor of variation of precompound decay parameters from those required for nonfissile systems.

I. INTRODUCTION

A great deal of experimental and nuclear modeling effort has been expended in order to deduce fission probabilities in actinide nuclei at excitations up to ≈ 12 MeV. In order to go beyond this excitation it is essential to consider explicitly the influence of preequilibrium decay prior to fission/evaporation competition. Several detailed comparisons of (α,xn) and fission yields on actinide targets (for α particles of up to 45 MeV) have been presented by Alexander and co-workers.[1-3]

The precompound formulation of the hybrid and geometry-dependent-hybrid (GDH) models was recently scrutinized to select a single global parameter set for nucleon-induced reactions.[4] Multiple precompound decay algorithms were included in the implementation of this parameter set in the code ALICE/LIVERMORE 82.[5] In the present work we wish to analyze ^{197}Au(α,xn) and ^{181}Ta(α,xn) excitation functions (for which there is no fission competition) and (α,xn) excitation functions on actinide targets using the new version of the precompound/compound codes. Parameters used in the precompound calculation will be those selected for nucleon-induced reactions, except that an initial exciton number appropriate for α-induced reactions will be substituted for the two-particle—one-hole value used for nucleon-induced reactions.

Our goal is to see the degree to which the present precompound codes reproduce the actinide results on an *a priori* basis, and therefore the degree to which they may be used as a future tool in deducing fissionabilities at excitations beyond the ≈ 12 MeV range. In Sec. II we will briefly discuss the precompound calculations which have been described in detail elsewhere.[4] The treatment and parameter selection for fission/evaporation competition in the actinide nuclei will also be presented in Sec. II. Comparisons of the (α,xn) excitation functions for the fissile and nonfissile systems are presented in Sec. III, and conclusions are given in Sec. IV.

The main emphasis of Refs. 1—3 was one of understanding the fission-evaporation competition in portions of the excitation functions for which compound nucleus reactions were dominant. The emphasis of the present work is rather on the portion of excitation functions where precompound processes are dominant. Our treatment of fission-evaporation competition will be much less sophisticated than that of Alexander *et al.*[1-3]

II. MODEL FORMULATION AND PARAMETERS

A. Precompound decay

The hybrid model[6] of precompound decay is given by

$$\frac{d\sigma}{d\epsilon}=\sigma_R \sum_{n=n_0}^{\bar{n}} \left[\frac{N_n^{\nu}(U,\epsilon)d\epsilon}{N_n(E)}\right]\left[\frac{\lambda_c(\epsilon)}{\lambda_c(\epsilon)+\lambda_+(\epsilon)}\right]D_n \ . \quad (1)$$

A detailed evaluation of the component quantities has been given elsewhere.[4] Briefly, σ_R is the reaction cross section; the quantity in the first set of parentheses gives the number of particle excitons of type ν (neutrons or protons) which are in an energy interval ϵ to $\epsilon+d\epsilon$ for an n exciton configuration. It may be shown that the expressions used may be derived on the basis of nucleon-nucleon scattering kinematics.[4] The second set of parentheses gives the fraction of the particles at excitation ϵ which should be emitted into the continuum. It consists of the rate of emission into the continuum, $\lambda_c(\epsilon)$, and the rate of intranuclear scattering, $\lambda_+(\epsilon)$. For the latter the Pauli corrected nucleon-nucleon scattering cross sections have been adopted for the global default option rather than using the imaginary optical potential which remains as a selectable option in the modified version of the ALICE code. This was done since the optical potential has not been accurately parametrized over the full range of energies of interest. The D_n factor represents the fraction of the initial population which has survived prior precompound decay.

In evaluating $\lambda_+(\epsilon)$ in the hybrid model an average nuclear density was used. This fails to take account of the important contributions of the diffuse nuclear surface region. Reactions in the surface should be limited in exciton hole depth versus reactions in bulk nuclear matter; longer mean free paths (mfp's) should also result in the diffuse surface region. It was shown that to first order

the effect of the longer mean free path in the surface could be handled in the formulation of Eq. (1) by doubling the average nucleon-nucleon mean free path.[7] To consider *both* surface effects (mfp and hole depth limit), Eq. (1) was reformulated (geometry dependent hybrid model), replacing σ_R by

$$\pi\lambda\!\!\!^{-2} \sum_{l=0}^{\infty} (2l+1)T_l ,$$

i.e., a sum over entrance channel trajectories with the remaining terms of (1) evaluated for the average density of each trajectory.[7] When this was done, the Pauli corrected nucleon-nucleon scattering cross sections were used *without* the factor of 2 multiplier to correctly reproduce experimental spectra and yields.

In modifying the precompound parameters for the ALICE/LIVERMORE 82 code only one significant change was made, primarily affecting the GDH model. This change was substitution of the Meyers droplet model[8] parametrization for the nuclear matter distribution, in place of the parameters from electron scattering which were sensitive to the nuclear charge distribution. We refer to Refs. 4, 9, and 10 for a quite detailed discussion of explicit evaluation of Eq. (1) and of the geometry dependent version.

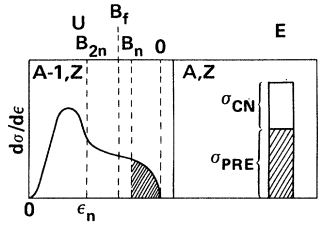

FIG. 1. Diagrammatic representation of the decay of the composite nucleus. The bar in the right-hand box indicates that a portion of the population of the composite nucleus A,Z at excitation E decays by precompound decay, while the remainder reaches equilibrium, decaying by an evaporation/fission competition mode. The spectral distribution in the left-hand box indicates the population by neutron emission due to the fast precompound mechanism, for which it is assumed that there is no fission competition. The one neutron out $(A-1,Z)$ nucleus cross section will approximately be given by the area under the spectrum corresponding to zero excitation up to an excitation corresponding to the lesser of the binding energy of one neutron or the fission barrier. It may be seen to be insensitive to fission parameters other than B_f if $B_f < B_n$. Decay at excitations above B_f, which would populate two or more neutron out products, may be seen to be strongly dependent on calculated fission probabilities competing with the equilibrium evaporation.

B. Fission/evaporation parameters

Following precompound decay (which we assume to be a fast process versus fission), the surviving compound nucleus cross section, and the populated daughter products (populated by precompound neutron and proton decay, either single or multiple) may either undergo particle evaporation or fission. In the code to be used, the Weisskopf evaporation model is used,[10] and it is assumed that photon emission does not compete when particle decay or fission channels are open. No provision is made in the code for "tunneling" below the classical fission barriers. Fission is treated by the Bohr-Wheeler transition state approach.[11]

The initial population features are illustrated in Fig. 1, where the daughter nuclei populated by precompound decay are indicated with their spectra of residual excitations. For the one neutron out product the neutron binding energy (B_n) and fission barriers (B_f) are indicated. For excitations up to B_f there can be no fission competition; this cross section will give the one neutron out yield (if $B_n > B_f$), which may therefore be seen to be sensitive to the shape and magnitude of the precompound spectrum, and quite independent of choice of equilibrium fission parameters.

Those parts of the residual excitation spectrum which may either emit one or more neutrons or undergo fission will either end up as 2n out (or more) products or as fission products. The branch between these channels will clearly be determined by the energy dependent fission parameters. Therefore success in reproducing the experimental (α,n) excitation functions primarily confirms success in correctly reproducing the cross section in the highest 5–6 MeV of the emitted (precompound) neutron spectrum, and the variation of this integral cross section with bombarding energy. Fitting the (α,xn) excitation functions for $x \geq 2$ requires either simultaneously correct precompound spectra and evaporation fission parameters, or a fortuitous combination of erroneous results for both. We will rely upon the level of success on fitting (α,xn) excitation functions for nonfissile nuclides to set a level of confidence for success in the actinide region, providing confidence that the fortuitous error choice is unlikely.

Fission barriers have been deduced for many of the nuclides of interest in this work via transfer reaction studies; results are summarized in Table I.[12–18] Fission probabilities versus excitation energy have been deduced from these experimental investigations. Our analyses via the ALICE/LIVERMORE 82 code uses the Bohr-Wheeler approach for estimating the rate of passage over the fission barrier, with a single barrier and no penetration below the barrier; where there is a two-humped barrier we replace the higher of these by the single barrier. Fermi gas level density formulas are used both for the saddle point and for the equilibrium nuclear particle evaporation.

Barrier heights used in calculations were based on the experimental results (Table I).[12–18] Because we had no fission barrier penetration in our code we used some barriers which were 0.2 to 0.3 MeV below the experimental values, but always within the expressed experimental uncertainties. We then adjusted the ratio of single particle level densities (saddle point to ground state, a_f/a_ν) by fitting calculated results to the published fission probabilities for isotopes for which results were available at excitations beyond 10 MeV.[12–17] These results are shown in Fig. 2. A value of a_f/a_ν of 1.12 was satisfactory for all Pu isotopes (237, 238, 239), and 1.15 was used for ^{239,240}Am. These values of a_f/a_ν were then used for calculation of excitation functions for production of all Pu and Am isotopes, respectively. The experimentally based barriers were read in as input to the ALICE/LIVERMORE 82

TABLE I. Fission parameters relevant to systems investigated in this work.

Nuclide	B_f^{expt} (MeV)		B_f^0 (MeV)[c]	B_f^{LD} (MeV)[d]	B_n (MeV)[e]	a_f/a_v[f]
	a	b				
^{239}Pu	6.2±0.2		6.0	4.5	5.6	1.12
^{238}Pu	5.5±0.2	6.2 ±0.2	5.5	4.4	7.0	1.12
^{237}Pu		5.60±0.3	5.3	4.3	5.9	1.12
^{236}Pu	4.5±0.4		4.5	4.2	7.3	1.12
^{235}Pu	5.1±0.4		5.1	4.1	6.3	1.12
^{234}Pu	5.8±0.7		5.8	4.0	7.8	1.12
^{233}Pu			6.4	3.9	6.4	1.12
^{241}Am	6.0±0.2	6.0 ±0.2	5.8	3.8	6.6	1.15
^{240}Am	6.5±0.2	6.15±0.2	6.1	3.7	6.0	1.15
^{239}Am	6.2±0.3	5.6 ±0.3	5.6	3.7	7.1	1.15
^{238}Am			5.4	3.6	6.3	1.15
^{237}Am			5.3	3.5	7.5	1.15

[a]Experimental fission barriers from Ref. 14 using the higher barrier of two.
[b]Experimental fission barriers from Ref. 18 using the higher barrier of two.
[c]Value used for fission barrier in this work in the Bohr-Wheeler approach at zero angular momentum.
[d]Liquid drop barrier results for zero angular momentum based on Cohen, Plasil, and Swiatecki, Ann. Phys. (N.Y.) 82, 55 (1979), as provided by default in the computer code used. These results were not used in these calculations and are listed only for comparison.
[e]Neutron binding energy.
[f]Ratio adopted for single particle levels at the fission barrier to those of the ground state nucleus.

code, and the option was selected which scaled these barriers with angular momentum in the same proportion as the rotating liquid drop model. These corrections were no more than 1 MeV over the relevant angular momentum ranges. We did not find experimental barrier information for ^{238}Am; we therefore used a value which scaled as the liquid drop result versus the experimental value for ^{239}Am (see Table I).

III. COMPARISONS OF CALCULATED AND EXPERIMENTAL EXCITATION FUNCTIONS

A. Nonfissile systems

Before applying precompound decay models to systems where yields are largely determined by fission-evaporation

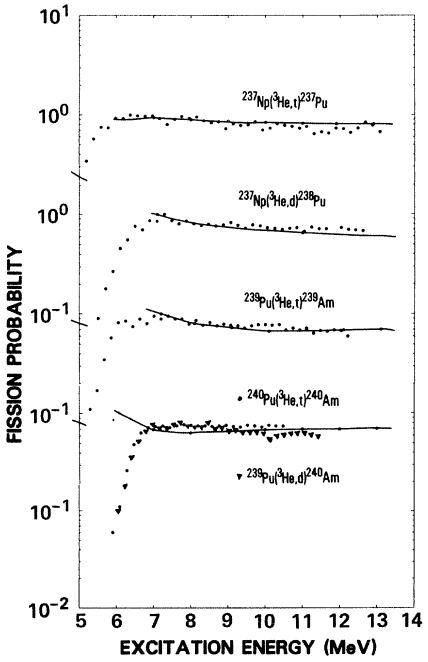

FIG. 2. Calculated versus experimentally deduced fission probabilities as a function of excitation energy. Experimental results are from Refs. 12–17. The solid line is the result of the evaporation/fission calculation using parameters as given in Table I.

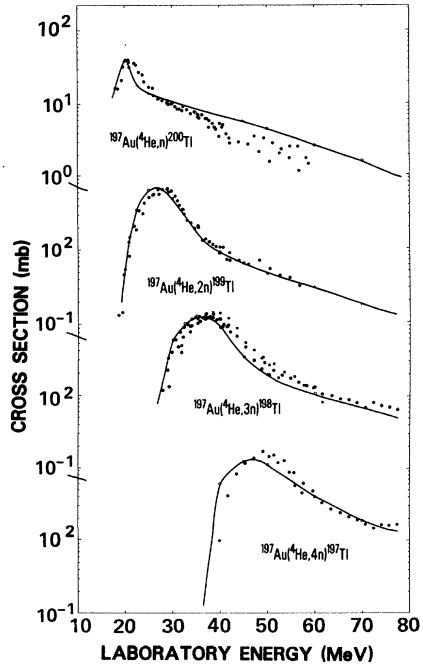

FIG. 3. Experimental and hybrid/evaporation model calculations for ^{197}Au(α,xn) excitation functions. Data are from Ref. 19. Calculated results are given by solid lines.

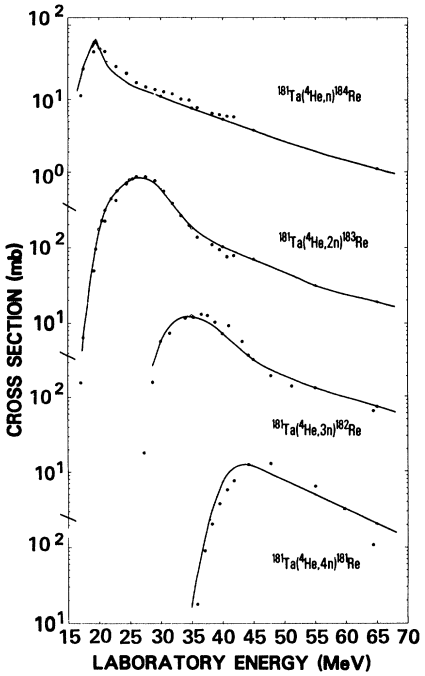

FIG. 4. As in Fig. 3, for ^{181}Ta(α,xn) excitation functions. Data are from Ref. 20.

competition, it is valuable to see how well or poorly the calculation does versus data without the additional complexity of fission. This approach was taken by Delagrange *et al.*,[3] and we analyze the same data, the (α,xn) yields of ^{197}Au (Ref. 19) and ^{181}Ta (Ref. 20), for α particle energies up to 80 MeV. Results are shown in Figs. 3 and 4. The region of comparison relevant to the actinide excitation functions extends up to 45 MeV ^{4}He energy.

The calculations for the nonfissile systems were performed using the hybrid model as recently modified in the ALICE/LIVERMORE 82 code.[4,5] Default options were used, except that the initial exciton number was input as four; two neutrons and two protons. Default options cause the nucleon-nucleon mean free path to be doubled over the *a priori* values based on free nucleon-nucleon scattering and the Pauli exclusion principle. This is not done for the geometry dependent hybrid model, which is used for calculations to be presented for actinide nuclei for which there is significant fission decay. The approximate equivalence of these two approaches, due to explicit treatment of the diffuse nuclear surface in one (GDH), was demonstrated previously.[7] Greater details of the precompound and evaporation calculations have been given elsewhere.[4]

It may be seen that most calculations agree with experimental results to within $\pm$(20—30)% in the precompound (tail) regions of the excitation functions. We would therefore expect the calculation to work reasonably well in the actinide region, degraded somewhat in quality by the additional requirement that the evaporation-fission competition be correctly reproduced.

B. Excitation functions for actinide products

Experimental and calculated (α,xn) excitation functions for $x=1$ to 3 on ^{233}U and $x=1$ to 4 on ^{234}U, ^{235}U, and ^{237}Np are shown in Figs. 5—8. The experimental results are from Refs. 1—3, as indicated in the figure captions.

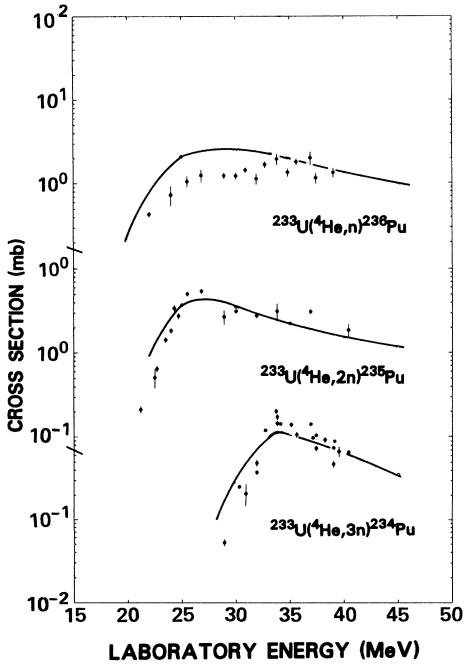

FIG. 5. Calculated and experimental ^{233}U(α,xn) excitation functions for $x=1$ to 3. Data are from Ref. 3. Calculations are given by solid lines and are as described in the text.

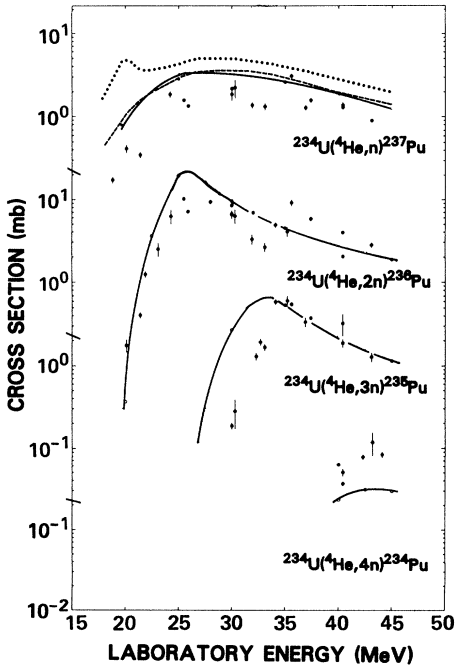

FIG. 6. As in Fig. 5 for ^{234}U(α,xn), $x=1$ to 4. The dotted curve is a result of a calculation in which fission probabilities were all set to zero; the dashed curve is the result of a calculation for which tabular fission probabilities based on experimental measurement were used as input.

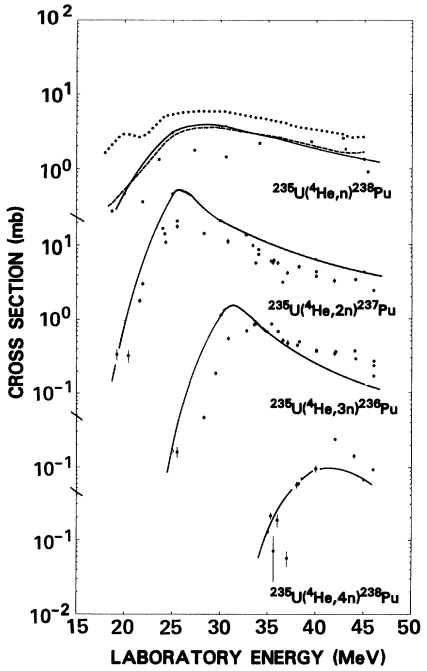

FIG. 7. As in Fig. 5 for $^{235}U(\alpha,xn)$, $x=1$ to 4.

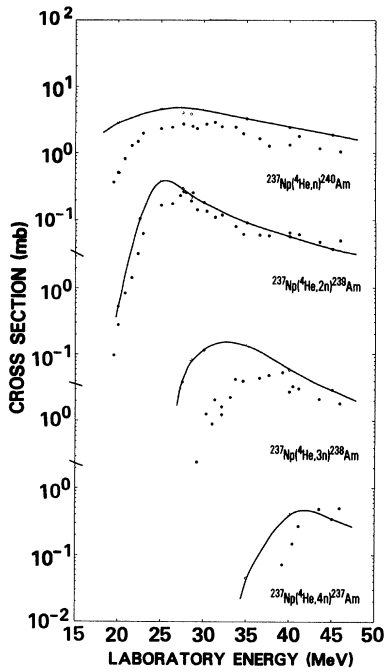

FIG. 8. As in Fig. 5 for $^{237}Np(\alpha,xn)$, $x=1$ to 4. Data are from Ref. 1.

The degree of success of the precompound decay calculation in reproducing the cross section which subsequently survives fission decay is found in comparing the high energy tails of calculated experimental excitation functions. The agreement is, to our judgment, good to excellent. Calculated results are to within a factor of 2 or better (mostly better) of experimental results, with the experimental scatter for several systems being comparable. That a constant value of a_f/a_ν over the 4n evaporation/fission cascade gives such a good result for the 4n excitation functions is surprising.

The precompound calculations performed include multiple precompound decay. However, this mode is unimportant at the excitations in Figs. 5—8. To verify this statement a set of calculations was performed for which the multiple precompound populations were set to zero, i.e., not stored. Results were indistinguishable from those presented in the figures. In an earlier work[4] it was shown that the multiple precompound decay algorithms work very well versus experimental results. We therefore believe that the conclusion in this case is strongly supported.

Some comments are in order on the lack of agreement between calculated and experimental excitation functions in the threshold regions. For the $^{237}Np(\alpha,n)$ excitation function the discrepancy may be immediately understood by comparing the experimental $(\alpha,f)+(\alpha,n)$ cross sections[1] at low α energy with the reaction cross sections generated by the parabolic model routine in the code used.[5] This comparison shows that the theoretical reaction cross sections which we used in the threshold region are much greater than the experimentally deduced values. Substitution of the experimental cross sections for the calculated reaction cross sections would bring the calculated $^{237}Np(\alpha,n)$ excitation function into excellent agreement with the experimental result in the threshold region. Some improvement would most likely also result in the (α,n) thresholds on U targets, if more accurate reaction cross sections were used in the near barrier region.

Another cause of uncertainty of calculated results in the near barrier region comes about from our crude treatment of fission probabilities in this region (see Fig. 2). To illustrate this point we have performed calculations with a modified version of the ALICE code in which tabular fission probabilities (based on experimentally deduced results) are used rather than Bohr-Wheeler statistically calculated results. We ran one set of calculations with this code version, and a second set in which fission probabilities were set to zero. Results for the (α,n) excitation functions are shown in Figs. 6 and 7 for these two sets of calculations. These comparisons show that fission competition modifies the calculated result over the entire excitation range, and dominates at α particle energies below $\approx$24 MeV. Discrepancies in calculated results in this range are more attributable to the treatment of evaporation-fission competition than of precompound decay. There is still a tendency to overestimate the (α,n) cross sections in the 25—35 MeV region. However, the pure precompound cross sections predicted in this range are in excellent agreement with the data. The discrepancy could lie in the fission probabilities used.

There are additional noticeable threshold shifts between the $^{234}U(\alpha,3n)$, $^{237}Np(\alpha,3n)$, and $^{237}Nb(\alpha,4n)$ experimental and calculated results; to a lesser degree this shows up in the $^{235}U(\alpha,3n)$ result as well. A part of this shift could be attributed to not having treated angular momentum either explicitly, or at least via the s-wave approximation. The latter shifts excitation functions to higher energies, reduces the threshold region slope, and decreases peak yields. Some additional decrease in peak yields might re-

sult from a calculation allowing tunneling through the fission barrier. For the ^{235}U(α,3n) case, data of Bethune *et al.*[21] are in excellent agreement with our calculations in the threshold region, suggesting that a part of these shifts might also represent experimental uncertainties. In spite of these threshold region shortcomings, the overall agreement of calculated and experimental excitation functions is quite good.

Reference 3 should be consulted for a more careful investigation of threshold cross sections, and, as mentioned earlier, of the fission evaporation which dominates excitation functions from the threshold to the peak yield region.

IV. CONCLUSIONS

We have applied the precompound plus evaporation model, with fission treated via the Bohr-Wheeler approach, to the analyses of (α,xn) excitation functions in the actinide region. Precompound parameters used were the set recently adopted for nucleon-induced reactions, except that for α-induced reactions the initial exciton number was taken to be four, two neutrons and two protons.

The pure precompound plus evaporation calculation was tested vs (α,xn) excitation functions on ^{181}Ta and ^{197}Au, for $x = 1$ to 4. The agreement was very good. Using barrier heights based on experimentally deduced results, we found values of a_f/a_ν which adequately reproduced experimentally deduced fission probability versus excitation results for some of the actinide nuclei produced in the α-induced reactions of interest. Using these results for barriers and a_f/a_ν, we calculated the actinide excitation functions including precompound decay. The results of these calculations gave quite satisfactory reproduction of the experimental data, without any parameter variation in particular in the regions dominated by precompound decay. We also found that multiple precompound decay, while included in our calculations, did not contribute significantly to the calculated results. We find no need to invoke pathological precompound decay parameters in order to reproduce experimental results as in Ref. 3, and conclude that the precompound formulation may be used as a valuable tool in deducing fission probabilities from experiments at moderate excitations. Insufficient detail is recoverable from Ref. 3 to understand reasons for differences in results. That work was, however, not principally focused on the precompound contributions, but rather on a sophisticated treatment of the fission/evaporation phenomena. Additionally, the precompound treatment of Ref. 3 largely explored approaches other than the hybrid model.

ACKNOWLEDGMENTS

The authors appreciate valuable communications from Prof. J. M. Alexander and Dr. H. Delagrange. This work was performed under the auspices of the U. S. Department of Energy by the Lawrence Livermore National Laboratory under Contract No. W-7405-ENG-48.

[1]S. Y. Lin and J. M. Alexander, Phys. Rev. C 16, 688 (1977); A. Fleury, F. H. Ruddy, M. N. Namboodiri, and J. M. Alexander, *ibid.* 7, 1231 (1973).
[2]J. Gilat, A. Fleury, H. Delagrange, and J. M. Alexander, Phys. Rev. C 16, 694 (1977).
[3]H. Delagrange, A. Fleury, and J. M. Alexander, Phys. Rev. C 17, 1706 (1978).
[4]M. Blann and H. Vonach, Phys. Rev. C 28, 1475 (1983).
[5]M. Blann and J. Bisplinghoff, Lawrence Livermore National Laboratory Report UCID-19614, 1982 (unpublished).
[6]M. Blann, Phys. Rev. Lett. 27, 337 (1971); 27, 700E (1971).
[7]M. Blann, Phys. Rev. Lett. 28, 757 (1972).
[8]W. D. Meyers, *Droplet Model of Atomic Nuclei* (IFI/Plenum, New York, 1977).
[9]M. Blann, Nucl. Phys. A213, 570 (1973).
[10]V. F. Weisskopf and D. H. Ewing, Phys. Rev. 57, 472 (1940).
[11]N. Bohr and J. A. Wheeler, Phys. Rev. 56, 426 (1939).
[12]B. B. Back, O. Hansen, H. C. Britt, and J. D. Garrett, Phys. Rev. C 9, 1924 (1974).
[13]B. B. Back, H. C. Britt, O. Hansen, B. Leroux, and J. D. Garrett, Phys. Rev. C 10, 1948 (1974).
[14]A. Gavron, H. C. Britt, E. Konecny, J. Weber, and J. B. Wilhelmy, Phys. Rev. C 13, 2374 (1976).
[15]P. D. Goldstone, H. C. Britt, R. Schoenmackers, and J. B. Wilhelmy, Phys. Rev. Lett. 38, 1262 (1977).
[16]H. C. Britt, S. C. Burnett, B. H. Erkkila, J. E. Lynn, and W. E. Stein, Phys. Rev. C 4, 1444 (1971).
[17]See references in the review by H. C. Britt, At. Data Nucl. Data Tables 12, 407 (1973).
[18]S. Bjornholm and J. E. Lynn, Rev. Mod. Phys. 52, 725 (1980).
[19]F. Lanzafame and M. Blann, Nucl. Phys. A142, 545 (1970).
[20]N. E. Scott, J. W. Cobble, and P. J. Daly, Nucl. Phys. A119, 131 (1968).
[21]G. R. Bethune, H. C. Britt, and B. H. Erkkila, Phys. Rev. C 6, 1087 (1972).